Growth and superconducting properties of $YBa_2Cu_3O_{7-\delta}$ films on conductive $SrRuO_3$ and $LaNiO_3$ multilayers for coated conductor applications

T. Aytug[a] and J. Z. Wu
Department of Physics and Astronomy, University of Kansas, Lawrence, Kansas 66045

C. Cantoni, D. T. Verebelyi, E. D. Specht, M. Paranthaman, D. P. Norton, and D. K. Christen
Oak Ridge National Laboratory, Oak Ridge, Tennessee 37831

R. E. Ericson and C. L. Thomas
3M Company, St. Paul, Minnesota 55144

(Received 8 November 1999; accepted for publication 13 December 1999)

Conductive multilayers of $YBa_2Cu_3O_{7-\delta}/SrRuO_3/LaNiO_3$ (YBCO/SRO/LNO), YBCO/SRO, and YBCO/LNO were grown epitaxially on single-crystal $LaAlO_3$ and $SrTiO_3$ substrates. Property characterizations revealed that the YBCO films on SRO and SRO/LNO buffer structures have excellent structural and superconducting properties. The YBCO/LNO, however, suffers degradation in superconducting transition temperatures and critical current densities, despite a good crystalline structure. The SRO/LNO bilayer showed excellent electrical contact with YBCO. These results have demonstrated the structural and chemical compatibility of SRO/LNO multilayers with YBCO and their potential use as conductive buffer layers for YBCO-based coated conductors as well as for other high-temperature superconducting applications. © *2000 American Institute of Physics.* [S0003-6951(00)04206-6]

Recently, development of the rolling-assisted biaxially textured substrates (RABiTS) process emerged as a promising method for the fabrication of $YBa_2Cu_3O_{7-\delta}$ (YBCO)-based coated conductors,[1,2] supporting high current for electric utility and high-magnetic-field applications operating at 77 K. The key issue in the RABiTS approach for conductor development is the necessity to use buffer-layer structures that are compatible with both the underlying metal substrate, Ni or Ni alloy, and YBCO. The function of the buffer layer is twofold. It prevents the diffusion of Ni to the superconductor and also transmits the biaxial texture of the metal substrate to the high-temperature superconducting (HTS) film. Ideally, conductive-oxide buffer layers are preferred for coated conductors as they can provide an electrical contact between the thin HTS layer and the thick underlying metal substrate, improving electrical stability in the event of a transient to the dissipative regime. To date, buffer-layer studies have mainly concentrated on insulating-oxide buffers and many multilayered buffers of insulating oxides have been developed for coated conductors.[1–4] Development of conductive-oxide buffer layers on RABiTS has just begun.[5]

In recent years, thin films of conductive oxide, $SrRuO_3$ (SRO), and $LaNiO_3$ (LNO) have attracted considerable interest due to their potential for many technological applications. For instance, their epitaxial growth made the development of heterostructures based on superconductors and ferroelectrics possible.[6–10] Both SRO and LNO are perovskite-type, conductive metallic oxides with pseudocubic lattice parameters of 3.93 and 3.83 Å with room-temperature resistivities of 280 and 540 $\mu\Omega$ cm, respectively. These values are close to those of orthorhombic YBCO and other high-temperature superconductors. It has been found that high-quality epitaxial YBCO thin films having high superconducting transition temperatures ($T_c = 91$ K) and critical-current densities ($J_c = 2\times10^6$ A/cm^2 at 77 K) can be grown on SRO-buffered single-crystal substrates.[11,12] However, to date there have not been any reports on the successful growth of SRO layers on textured metals for the development of YBCO-based coated conductors. On the other hand, He *et al.* reported recently growth of YBCO films on highly textured LNO buffer layers, successfully deposited onto Ni tapes.[5] These YBCO films showed depressed T_c values around 75–80 K, consistent with earlier results of YBCO films on LNO-buffered single-crystal substrates.[13,14] In Ref. 5, the reason for this degradation was attributed to two possibilities: (1) direct chemical reaction between YBCO and LNO and (2) diffusion of Ni through the LNO layer into the YBCO. Hence, the observations that SRO is compatible with YBCO and LNO is compatible with RABiTS has motivated the present study of SRO/LNO multilayers for possible application as a conductive buffer-layer structure for YBCO-based coated conductors. In this letter, we have made a comparative study of the structural and the superconducting properties (T_c, J_c) of YBCO films grown on multilayers of SRO/LNO and on single-layer LNO, SRO-buffered (100)-oriented $LaAlO_3$(LAO) and $SrTiO_3$(STO) substrates.

The deposition of LNO buffer layers was performed with a rf-magnetron sputtering system using a single-phase LNO powder target, which was pressed into a 95 mm copper tray. Typical sputtering conditions consist of a mixture of Ar and O_2 at a ratio of $Ar/O_2 = 15/2$, with a total pressure of 10 mTorr and a substrate temperature in the range of 550–

[a]Electronic mail: aytug@eagle.cc.ukans.edu

 © 2000 American Institute of Physics
Downloaded 06 Sep 2009 to 160.91.157.167. Redistribution subject to AIP license or copyright; see http://apl.aip.org/apl/copyright.jsp

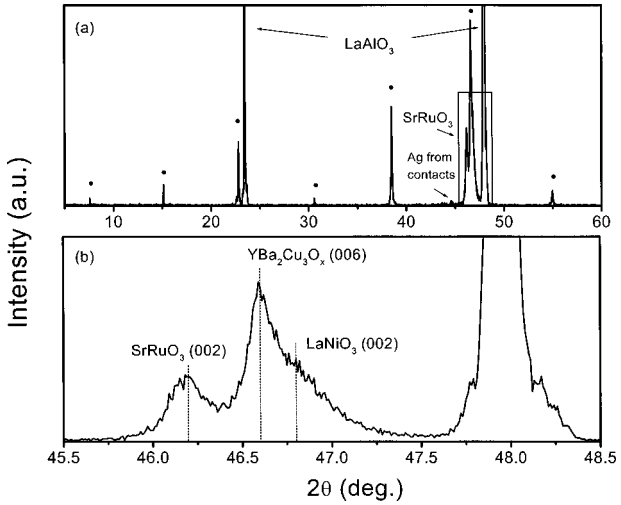

FIG. 1. XRD θ–2θ scan for the (a) YBCO/SRO/LNO/LAO multilayer. YBCO(00l) peaks are indicated by (●). The weak Ag peak is due to electrical contacts. (b) The LNO(002) scattering can be seen from the enlargement of the boxed region.

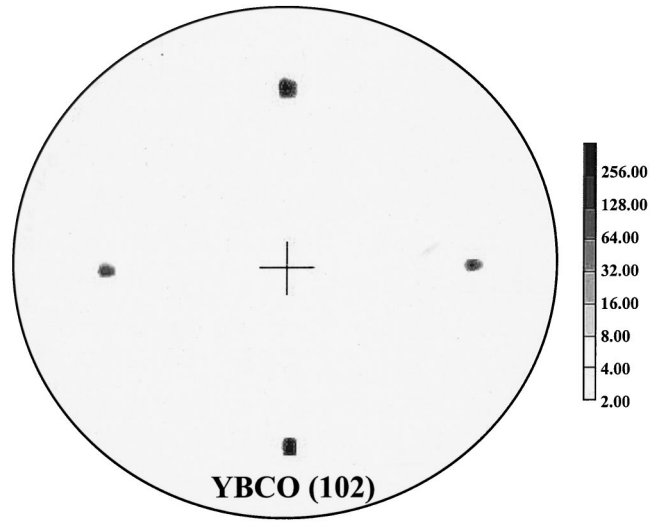

FIG. 2. Logarithmic scale (102) pole figure of YBCO grown on SRO/LNO/LAO multilayer.

600 °C. The deposition rate was ~0.42 Å/s with a corresponding film thickness of about 3000 Å.

Pulsed-laser deposition (PLD) was employed for the deposition of SRO as well as the YBCO films. A KrF excimer laser system operated with an energy density of ~3 J/cm^2 was used. During the deposition of SRO layers the substrates were kept at 600 °C in an O_2 atmosphere of 5 mTorr. The deposition of YBCO films was achieved at 780 °C in 100 mTorr of O_2. After deposition, the O_2 pressure inside the PLD chamber was increased to 500 Torr and the films were then cooled to room temperature at a rate of 10 °C/min. Typical film thicknesses for SRO and YBCO were 2000 and 3000 Å, respectively. The structures of the films were characterized with a Huber high-resolution x-ray diffractometer (XRD). A standard four-probe technique was used to evaluate the electrical properties of the samples. The values of J_c were assigned using a 1 μV/cm criterion. Silver contacts were deposited onto the samples using dc-magnetron sputtering followed by an O_2 annealing in 1 atm for 30 min at 500 °C. Secondary-ion-mass-spectrometry (SIMS) depth-profile measurements and inductively coupled plasma (ICP) analysis of the samples were also made to document possible cation contamination of the YBCO.

An XRD θ–2θ spectrum for a typical YBCO film on a SRO/LNO/LAO multilayer structure is shown in Fig. 1(a). The pattern indicates only (00l) reflections from both the YBCO and SRO layers, demonstrating that the YBCO/SRO/LNO are c-axis oriented. The LNO (002) reflection can be seen as a shoulder on the YBCO (006) peak from the enlargement of the boxed region, as shown in Fig. 1(b). The epitaxial relation of the YBCO films on the substrates is determined by XRD pole figure analysis. The logarithmic scale (102) pole figure of a YBCO film on SRO/LNO/LAO, shown in Fig. 2, indicates a single epitaxy with YBCO(001)‖substrate(001) and YBCO(110)‖substrate(110). Similar crystallographic relations were observed for the YBCO/SRO/LNO/STO, YBCO/LNO/(LAO and STO), and YBCO/SRO/LAO multilayer structures.

The differences in electrical and superconducting properties of the multilayer samples can be seen from the temperature-dependent resistivity curves in Fig. 3, with an inset showing the enlarged view of the transition region. For comparison, the result of a YBCO film on a STO substrate is included. Note that Fig. 3 shows the net resistivity (ρ_{net}), which is calculated from the total thickness of the conductive (YBCO+buffer layers) structure. It is clear that an additional SRO buffer layer on LNO/(LAO and STO) improves the superconducting properties of the YBCO films by increasing T_c and decreasing ρ_{net}. The T_c of the YBCO/SRO/LNO/(LAO and STO) samples was observed to be higher than 90 K, being close to the $T_c = 92$ and 91 K values of the YBCO films grown on single-crystal STO- and SRO-buffered LAO substrates, respectively. However, T_c of the YBCO/LNO/(LAO and STO) were lower than 90 K, with normal-state ρ_{net} being 3–4 times higher than those of YBCO/SRO/LNO/(LAO and STO). The differences in these results suggest the possible Ni contamination of the YBCO films from the LNO layers. In fact, SIMS depth-profile measurements and ICP analysis of YBCO/LNO/(LAO and STO) samples qualita-

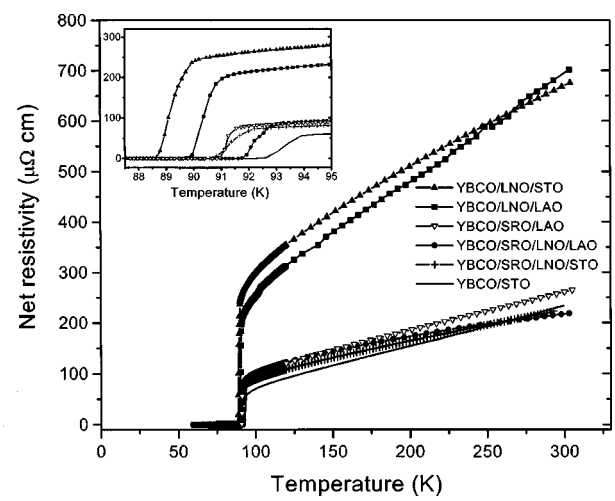

FIG. 3. Temperature dependence of the net resistivity of YBCO/SRO/LNO/(LAO and STO), YBCO/LNO/(LAO and STO), YBCO/SRO/LAO, and YBCO/STO structures. Inset shows the enlarged view of the superconducting transition region.

Downloaded 06 Sep 2009 to 160.91.157.167. Redistribution subject to AIP license or copyright; see http://apl.aip.org/apl/copyright.jsp

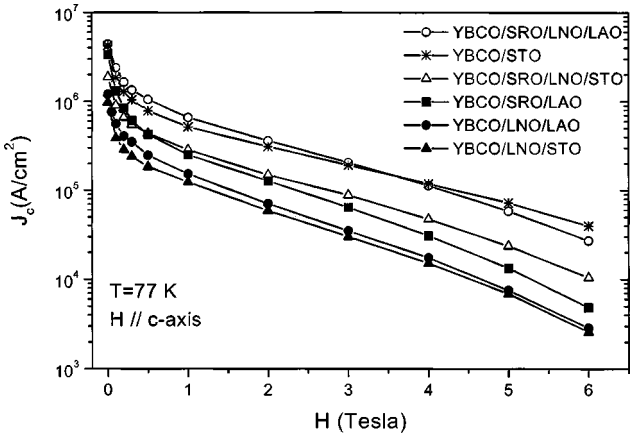

FIG. 4. Magnetic-field dependence of J_c of YBCO/SRO/LNO/(LAO and STO), YBCO/LNO/(LAO and STO), and YBCO/SRO/LAO multilayers at 77 K. For comparison, J_c data of YBCO/STO are also included.

tively confirmed the presence of Ni in the YBCO. It is well known that Ni impurities in the superconducting structure can significantly reduce T_c and increase ρ.[15] The expression for the resistivity ratio ρ_{net}/ρ_Y, of an electrically connected bilayer structure can be given by $\rho_{\text{net}}/\rho_Y=[(A_Y+A_B)/(A_Y+(\rho_Y/\rho_B)A_B)]$, where A_Y,ρ_Y, and A_B,ρ_B are the cross-sectional areas and the resistivities of the YBCO and the conductive buffer-layer structures, respectively. According to this expression, ρ_{net}/ρ_Y is always >1 if $\rho_B>\rho_Y$, and <1 if $\rho_B<\rho_Y$. Since $\rho_Y\approx 300\ \mu\Omega$ cm and $\rho_{\text{SRO}}\approx\rho_{\text{LNO}}\approx\rho_Y$, we should expect $\rho_{\text{net}}\approx\rho_Y$. Indeed, in contrast to YBCO films on LNO layers where Ni contamination is an issue, the fact that ρ_{net} of the YBCO/SRO/LNO multilayer is similar to ρ_{net} of the YBCO on STO, and comparable to the one on SRO/LAO, is an indication of excellent electrical contact among all three layers. It is also noted that the T_c values of samples on LAO substrates appear to be ≈ 2 K higher than that of samples on STO substrates, suggesting that LAO serves as a marginally better substrate for growth of such buffer-layer structures. Confirmation of this effect needs further investigation.

Figure 4 shows the magnetic-field dependence of the transport J_c for these samples at 77 K, with the field applied parallel to the c axis. At zero applied field, all samples support high $J_c\geqslant 1.0\times 10^6$ A/cm^2, with irreversibility fields $(H_{\text{irr}})\geqslant 6$ T. Consistently high J_c performance was observed for samples on SRO layers. Specifically, the self-field J_c of the YBCO/SRO/LNO/LAO is near 4.4×10^6 A/cm^2 with a high H_{irr} of 7.5 T (data not shown in the plot for consistency). These values are comparable to those of the benchmark films of YBCO/STO ($J_c=4.4\times 10^6$ A/cm^2, $H_{\text{irr}}=8$ T), and confirms high-quality epitaxial growth of YBCO on SRO/LNO multilayers. However, the YBCO/LNO/(LAO and STO) multilayer structures showed somewhat lower J_c values (1.4×10^6 and 1×10^6 A/cm^2) with $H_{\text{irr}}\cong 6$ T. This is also consistent with the lower T_c values observed for the YBCO films on LNO layers. These results further support the low-level contamination of YBCO through LNO layers. It should also be mentioned that similar to the observations made in the ρ_{net} vs T data, J_c values of YBCO films on LAO substrates are also slightly higher than those on STO substrates.

In summary, structural and superconducting properties of conductive multilayer structures of YBCO/SRO/LNO, YBCO/SRO, and YBCO/LNO grown on LAO and/or STO substrates have been investigated. Highly crystalline, low-resistivity, and chemically compatible YBCO/SRO/LNO/(LAO and STO) samples have been obtained. The T_c and J_c of YBCO films on SRO/LNO multilayers have showed significantly higher values than those of the YBCO films grown on single LNO layers. These results indicate that the observed low-level Ni contamination of YBCO through the LNO layer can be prevented by an additional, highly stable SRO layer. This work also points to the use of the SRO/LNO structure as a potential buffer-layer architecture for the development of RABiTS-based, fully conductive YBCO-coated conductors.

Research was cosponsored by the DOE Division of Materials Sciences, and by the DOE Office of Power Technologies, both under Contract No. DE-AC05-96OR22464 with Lockheed Martin Energy Research Corp. Two of the authors (T. A. and J. Z. W.) would like to acknowledge NSF Grant No. DMR-9901460 and AFOSR Grant No. F49620-96-1-0358.

[1] A. Goyal, D. P. Norton, J. D. Budai, M. Paranthaman, E. D. Specht, D. M. Kroeger, D. K. Christen, Q. He, B. Saffian, F. A. List, D. F. Lee, P. M. Martin, C. E. Klabunde, E. Hatfield, and V. K. Sikka, Appl. Phys. Lett. **69**, 1795 (1996).
[2] D. P. Norton, A. Goyal, J. D. Budai, D. K. Christen, D. M. Kroeger, E. D. Specht, Q. He, B. Saffian, M. Paranthaman, C. E. Klabunde, D. F. Lee, B. C. Sales, and F. A. List, Science **274**, 755 (1996).
[3] C. M. Carlson, J. C. Price, P. A. Parilla, D. S. Ginley, D. Niles, R. D. Blaugher, A. Goyal, M. Paranthaman, D. M. Kroeger, and D. K. Christen, Physica C **304**, 82 (1998).
[4] M. Paranthaman, D. F. Lee, A. Goyal, E. D. Specht, P. M. Martin, X. Cui, J. E. Mathis, R. Feenstra, D. K. Christen, and D. M. Kroeger, Supercond. Sci. Technol. **12**, 319 (1999).
[5] Q. He, D. K. Christen, R. Feenstra, D. P. Norton, M. Paranthaman, E. D. Specht, D. F. Lee, A. Goyal, and D. M. Kroeger, Physica C **314**, 105 (1999).
[6] C. B. Eom, R. B. Van Dover, J. M. Philips, D. J. Werder, J. H. Marshall, C. H. Chen, R. J. Cava, R. M. Fleming, and D. K. Fork, Appl. Phys. Lett. **63**, 2570 (1993).
[7] C. H. Ahn, R. H. Hammond, T. H. Geballe, M. R. Beasley, J.-M. Triscone, M. Decroux, Ø. Fisher, L. Antognazza, and K. Char, Appl. Phys. Lett. **70**, 206 (1997).
[8] C. C. Yang, M. S. Chen, T. J. Hong, C. M. Wu, J. M. Wu, and T. B. Wu, Appl. Phys. Lett. **66**, 2643 (1995).
[9] L. Antognazza, K. Char, T. H. Geballe, L. L. H. King, and A. W. Sleight, Appl. Phys. Lett. **63**, 1005 (1993).
[10] R. Dömel, C. L. Jia, C. Copetti, G. Ockenfuss, and A. I. Braginski, Supercond. Sci. Technol. **7**, 277 (1994).
[11] X. D. Wu, S. R. Foltyn, R. C. Dye, Y. Coulter, and R. E. Muenchausen, Appl. Phys. Lett. **62**, 2434 (1993).
[12] P. Tiwari, X. D. Wu, S. R. Foltyn, M. Q. Le, I. H. Campbell, R. C. Dye, and R. E. Muenchausen, Appl. Phys. Lett. **64**, 634 (1994).
[13] K. M. Satyalakshmi, R. M. Mallya, K. V. Ramanathan, X. D. Wu, B. Brainard, D. C. Gautier, N. Y. Vasanthacharya, and M. S. Hegde, Appl. Phys. Lett. **62**, 1233 (1993).
[14] M. Sagoi, T. Kinno, J. Yoshida, and K. Mizushima, Appl. Phys. Lett. **62**, 1833 (1993).
[15] Y. Maeno, T. Nojima, Y. Aoki, M. Kato, K. Hoshino, A. Minami, and T. Fujita, Jpn. J. Appl. Phys., Part 2 **26**, L774 (1987).

Downloaded 06 Sep 2009 to 160.91.157.167. Redistribution subject to AIP license or copyright; see http://apl.aip.org/apl/copyright.jsp